Synthesis, characterization, and theoretical analysis of a plutonyl phosphine oxide complex

DOI:
10.1039/d1dt03041h

Document Version
Accepted author manuscript

COMMUNICATION

Synthesis, characterization, and theoretical analysis of a plutonyl phosphine oxide complex†

Received 00th January 20xx,
Accepted 00th January 20xx

DOI: 10.1039/x0xx00000x

Cory J. Windorff,[a,b]* Maria J. Beltran-Leiva,[a] Thomas E. Albrecht-Schönzart,[a] Zhuanling Bai,[a] Cristian Celis-Barros,[a]* Conrad A. P. Goodwin,[c,d] Zachary Huffman,[a] Noah C. McKinnon,[a] and Joseph M. Sperling[a]

The synthesis of *trans*-$PuO_2Cl_2(OPcy_3)_2$, 1-Pu, has been carried out and confirmed by single crystal X-ray diffraction along with UV-vis-NIR, and ^{31}P NMR spectroscopies. Theoretical analysis finds that despite a higher calculated covalency for the Pu–Cl interaction, the Pu–$OPcy_3$ interaction is stronger due to the accumulation of electron density in the interatomic region. The coordination of equatorial ligands slightly decreases the strength of the Pu≡O_{yl} interactions relative to the free gas phase $(PuO_2)^{2+}$ ion.

Phosphine oxides play a critical role in the recycling and separations of actinides e.g. the **p**lutonium **ur**anium **r**eduction **ex**traction (PUREX) process.[1, 2] The structural and extraction behaviour of uranium-phosphine oxide compounds is well defined, in particular as the uranyl ion, $(UO_2)^{2+}$.[3] However, the structural chemistry of the transuranium actinyl compounds is far less developed with just a handful of Np^{VI}/Pu^{VI} complexes that have been structurally characterized in the form $AnO_2X_2(OPPh_3)_2$, or $[AnO_2(OPPh_3)_4][X']_2$ (X = Cl, NO_3; X′ = ReO_4, ClO_4).[4-9] Recent examination of its saturated analogue, $OPcy_3$ (cy = cyclohexyl, C_6H_{11}) in *mer*-$M^{III}Br_3(OPcy_3)_3$ (M = Am, La – Nd) showed an unusual amount of metal-based pseudo-core 5p/6p participation in bonding with the $OPcy_3$ ligand.[10] The difference in saturation not only affects the steric profile of the molecules, but also the donation strength of the phosphine oxide, *via* differing electronic structure.[11] The $OPcy_3$ ligand has been shown to be a stronger donor than $OPPh_3$ for actinyl ions, $(An^{VI}O_2)^{2+}$ (An = U, Np) but can be displaced by $HNPcy_3$ or $HNPPh_3$.[5-7, 12, 13] Although a synthesis of $PuO_2Cl_2(OPcy_3)_2$ has been reported as a conference proceeding that included a summary of the synthesis and the ^{31}P NMR spectroscopy resonances, but not the solvent.[12] Because of the uncertainty of the structural and in depth spectroscopic details of $PuO_2Cl_2(OPcy_3)_2$, we sought to re-examine it. Herein we continue the study of $OPcy_3$ with actinide complexes through structural, spectroscopic, and theoretical studies of *trans*-$PuO_2Cl_2(OPcy_3)_2$.

We began our investigation by revisiting and scaling down analogous uranyl chemistry using 15-20 mg of metal content, typical of plutonium chemistry. When a solution of OPR_3 (R = cy, Ph) was carefully layered on top of a solution of $UO_2X_2•nH_2O$ in a polar solvent (EtOH for X = Cl; Acetone for X = NO_3), bright yellow X-ray quality crystals of *trans*-$UO_2Cl_2(OPcy_3)_2$, **1-U**, *trans*-$UO_2Cl_2(OPPh_3)_2$, **2-U**, *trans*-$UO_2(NO_3)_2(OPcy_3)_2$, **3-U**, and *trans*-$UO_2(NO_3)_2(OPPh_3)_2$, **4-U**, grew upon standing overnight, see ESI for synthetic details. While the structure of **1-U•DCM** is known with a lattice DCM solvent molecule, synthesis in ethanol gave **1-U** as the solvent free crystal structure featuring two crystallographically independent units, which both feature an inversion centre in the $P\bar{1}$ space group. The bond metrics of **1-U** compare well with **1-U•DCM**,[5] as well as with the $OPPh_3$ analogue, **2-U**, see ESI for comparisons.[14, 15] Complex **3-U** is a new molecule and displays the anticipated 8-coordinate, distorted hexagonal bipyramidal geometry of similar complexes, such as the known $OPPh_3$ analogue **4-U**.[16]

With this chemistry in hand, we extended our synthesis to plutonium, starting from freshly generated $PuO_2Cl_2(H_2O)_x$. A solution of $PuO_2Cl_2(H_2O)_x$ in methanol was carefully layered with a solution of $OPcy_3$ in ethanol, and upon slow evaporation of the solvent pale-yellow crystals of *trans*-$PuO_2Cl_2(OPcy_3)_2$, **1-Pu**, formed. This was confirmed by single crystal X-ray crystallography, **Fig. 1**, **eq. 1**. **1-Pu** was isolated in high yield following work up, and the sample was brought into a negative pressure glovebox dedicated to actinide chemistry. **1-Pu** is isomorphous with **1-U** crystallizing in the same $P\bar{1}$ space group with two crystallographically independent units, each with one

[a] *Department of Chemistry and Biochemistry, Florida State University, 95 Chieftan Way, RM. 118 DLC, Tallahassee, Florida 32306, United States of America.* **E-mail: ccelisbarros@fsu.edu*
[b] *Department of Chemistry and Biochemistry, New Mexico State University, MSC 3C, PO Box 3001, Las Cruces, NM 88003, United States of America.* **E-mail: windorff@nmsu.edu*
[c] *Chemistry Division, Los Alamos National Laboratory, Los Alamos, NM 87545, United States of America.*
[d] *Current Address: Department of Chemistry, School of Natural Sciences, The University of Manchester, Oxford Road, Manchester, M13 9PL, United Kingdom.*

†Electronic Supplementary Information (ESI) available: Synthesis of compounds, photographs of compounds, UV-vis-NIR and NMR spectra, extended computational tables, and crystallographic details in CIF format. CCDC 2101627–2101630. See DOI: 10.1039/x0xx00000x

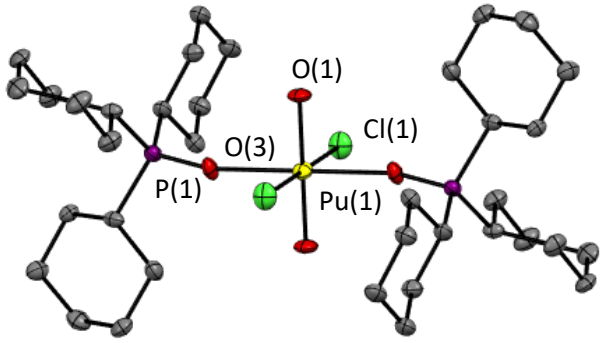

Fig. 1. Thermal ellipsoid plot of one crystallographically independent unit of **1-Pu**, drawn at the 50% probability level with hydrogen atoms omitted for clarity, only non-carbon atoms in the asymmetric unit are labelled. Isomorphous **1-U** is depicted in **Fig. S18**.

half of a molecule present in the asymmetric unit. The geometry is best described as a distorted octahedron where all of the homo-ligands have a rigorous 180° bond angle due to the crystallographic inversion centre. The O_{yl}–Pu–Cl and O_{yl}–Pu–O_P bond angles for the two independent units range from 88.4(1) to 91.6(1)°, see **Table S7** for further details. The Pu–Cl bonds are distinct between the two independent molecules, with lengths of 2.633(2) and 2.652(2) Å. This difference in Pu–Cl bond lengths come with a complementary, but not significant (using the 3σ criteria), difference in Pu–O_P with bond lengths of, 2.301(4) and 2.281(5) Å. The Pu≡O_{yl} bond lengths are 1.762(4) and 1.742(4) Å. These bond metrics compare well with the previously reported structure of *trans*-$PuO_2Cl_2(OPPh_3)_2$,[7] **2-Pu**, where the Pu≡O_{yl} bond length was 1.747(4) Å, the Pu–Cl bond length was 2.630(2), and the Pu–O_P bond length was 2.302(4) Å, see **Table S8** for a full comparison.

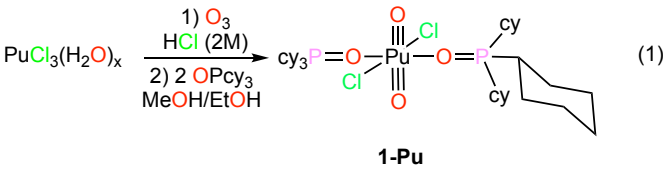

(1)

1-Pu

To better understand the bonding in **1-Pu** and **1-U** we turned to Complete Active Space Self Consistent Field (CASSCF) calculations to generate the corresponding molecular densities for analysis by Bader's Quantum Theory of Atoms in Molecules (QTAIM).[17] The active space consisted of n electrons in 10 orbitals for the CAS (n,10) calculations on **1-Pu** (n = 8) and **1-U** (n = 6). To keep the structure imposed by the crystal packing, the coordinates from the crystal structure were used for the calculations without optimization, see ESI for further details. The corresponding gas phase $(AnO_2)^{2+}$ ions have been also considered as reference. In the QTAIM formalism, the chemical bond is understood by analysing changes in the electron density, ρ(r), as well as the delocalization index, δ(r), at the bond critical point (BCP). Increases in ρ(r) are associated with increased covalency and results in a strengthening of the bond. This is accompanied by an increase in the δ(r), which is considered as an alternative bond-order descriptor.[17] Conversely, changes in δ(r) can also be related to an increase in covalency without a change in the strength of the bond. The elucidation of the nature of the bond is further supported by the energy parameters derived from potential, V(r), kinetic, G(r), total H(r), energy densities. Where V(r) signifies a stabilization of electron density at the BCP, while G(r) signifies destabilization due to an excess of kinetic energy at the BCP. Therefore, a negative H(r) value corresponds to a quantification of covalent interactions.[18, 19] By normalizing the values, H(r)/ρ(r), a "covalency degree" is obtained, and functions as a more general description of covalency.[18]

For the sake of clarity, the discussion of the bonding in **1-U** and **1-Pu** will be addressed as a perturbation of the gas phase $(AnO_2)^{2+}$ ion. The interaction between An(VI) (An = U, Np, Pu) centres and oxo ligands has been widely studied, where Raman spectroscopy unequivocally suggests that the U≡O_{yl} bonds are stronger than Pu≡O_{yl}.[20] Conversely, an accurate theoretical interpretation of experimental XANES spectra suggests otherwise.[21] As expected, the $(AnO_2)^{2+}$ ions shows similar bonding patterns, i.e. a triple An≡O_{yl} bond based on the zero-valued bond ellipticities, ε(r).§ However, the increased accumulation of ρ(r) and greater δ(r) suggests the Pu≡O_{yl} bonds in $(PuO_2)^{2+}$ to be more covalent than the U≡O_{yl} bonds of $(UO_2)^{2+}$, **Table S3**. Due to electron correlation, the estimated bond orders, based on the δ(r) values, deviate significantly from a triple bond with values of 1.35 and 1.50 for $(UO_2)^{2+}$ and $(PuO_2)^{2+}$, respectively, **Table S3**. It is noteworthy that though H(r) favours $(PuO_2)^{2+}$ as the most covalent complex, the values of the covalency degree indicate that the electrons of $(UO_2)^{2+}$ are more covalently bound in $(UO_2)^{2+}$, illustrating the complex nature of the term "most covalent." This further raises the question of: What metrics relate better to bond strength? While the H(r) values correlate with the XANES interpretation, the covalency degree value agrees with the Raman measurements. This highlights the complex interplay of covalency, bond order, and bond strength in actinyl compounds.

According to the QTAIM metrics the coordination of the Cl^{1-} and $OPcy_3$ ligands in the equatorial plane weaken the An≡O_{yl} bonds in both **1-U** and **1-Pu**, relative to $(UO_2)^{2+}$ and $(PuO_2)^{2+}$, respectively. This weakening is quantified as ΔAn≡O_{yl}, where the effect is more strongly observed in **1-U** than in **1-Pu**, **Table S3**. The perturbation of the An≡O_{yl} bonds upon coordination of the Cl^{1-} is rather similar for both complexes, but the most significant weakening of the U≡O_{yl} bonds is due to the coordination of the $OPcy_3$ ligands, given as ΔAn–L in **Table S3**. The weakening of the An≡O_{yl} interaction is on the order of 12% and 6% [based on ρ(r)] for U and Pu, respectively. This weakening is shown by the significant reduction of the ρ(r), δ(r), and H(r) values at the U≡O_{yl} BCP in **1-U** relative to the $(UO_2)^{2+}$ ion. Furthermore, the ε(r) of **1-U** deviates more significantly from zero than in **1-Pu**, supporting the claim of weaking the U≡O_{yl} interaction, **Table S3**.

As expected, the calculated bond covalency follows the charge of the ligand, O^{2-} >> Cl^{1-} > $OPcy_3$, **Table S3**. It is important to note that despite the larger covalent character predicted for the An–Cl bonds (greater total energy densities), the An–$OPcy_3$ bonds are *stronger* (greater electron densities). This is also one

example showing that covalency does not necessarily correlate with bond strength.

To further understand these differences, Natural Localized Molecular Orbitals (NLMOs) have been calculated from the scalar relativistic CASSCF densities. NLMOs break down bonding interactions into the component orbitals, both from the bonding atoms, as well as the contributing orbital hybrids from each atom. Notably the NLMOs of the metal 6p_z orbital display polarization of the semi-core electron density towards the 5*f* shell, where $(PuO_2)^{2+}$ > $(UO_2)^{2+}$, with 19% and 14% mixing, respectively, which is fundamental for the strengthening of the U≡O_{yl} bonds in the so-called "Inverse Trans Influence" (ITI), **Fig. S15**.[22] This polarization is reduced significantly upon the coordination of equatorial ligands to 6% (**1-Pu**), and 14% (**1-U**), suggesting that $(UO_2)^{2+}$ is more sensitive to ligand coordination, as also shown by the QTAIM metrics. The NLMO analysis also confirmed the An≡O_{yl} interaction to be a triple bond consisting of one σ-type and two π-type bonds for all species, **Fig. S15**. Decomposition of the NLMOs indicates that the orbital hybrids are dominated by the 5*f* over the 6*d* orbitals. With $(UO_2)^{2+}$ again displaying increased sensitivity to ligand coordination over $(PuO_2)^{2+}$, as confirmed by: the occupation numbers, the contributions to the total bond order, and the hybrid overlaps, **Fig. S15** & **Table S4**.

Examination of the bonding in the equatorial ligands suggests that the 6*d* orbitals dominate the NLMO compositions, with nearly equal contributions from 5*f* and 7*s* orbitals in the σ–based NLMOs. The better energy match between the actinide centre and the Cl–3*p* orbitals compared to O_p–2*p* orbitals yields reduced polar bonds of the An–Cl interaction giving similar values for both **1-Pu** and **1-U**, i.e. ~12% metal contribution (~88% polar) versus 6% (94% polar), respectively, **Fig. 2**. This agrees with the predicted V(r)/G(r) polarization values for these two bond types by QTAIM, ~81% and ~93%, for **1-U** and **1-Pu**, respectively, **Table S3**. We note that there is a very small amount of metal based π–contribution to the bonding as well, 2–5% depending on the symmetry and the identity of the ligand, Cl^{1-} vs. $OPcy_3$, see **Fig. S16**. Interestingly, no semi-core 6*p* orbital involvement was found in the An–O_P interactions, compared to previous results with *mer*-$MBr_3(OPcy_3)_3$ (M = Am, Nd, Ce).[10] An overall agreement between localized orbitals and QTAIM is observed. However, the former fails to recover the increased orbital overlap in the An–O_P bonds with respect to the An–Cl bonds, as predicted by QTAIM.

The takeaway message from the bonding analysis is that the coordination of Cl^{1-} and $OPcy_3$ ligands to $(UO_2)^{2+}$, forming **1-U**, affects the U≡O_{yl} interaction more significantly than the $(PuO_2)^{2+}$/**1-Pu** analogues. It is also observed that the $OPcy_3$ ligands have a stronger bonding interaction with the metal *despite* more covalent character of the U–Cl and Pu–Cl bonds, **Table S3**.

Turning to the solid-state electronic absorption spectroscopy of **1-Pu**, the spectrum displays several weak excitations in the range of ~13,000–10,000 cm^{-1} (~760–1000 nm) and a broad charge transfer band >24,000 cm^{-1} (<400 nm). The characteristic excitation at ~12,050 cm^{-1} (831 nm) for $(PuO_2)^{2+}$ in 1M $HClO_4$ is not present in **1-Pu**, **Fig. 3**.[3] Attempts to record a solution phase spectrum showed evidence of reduction to Pu(IV), see **Fig. S5**. To help explain the electronic structure and spectroscopic properties of **1-Pu** and **1-U**, we employed spin-orbit (SO) CASSCF wavefunctions corrected by second order perturbation theory (PT2) compared with the gas-phase actinyl dications, $(AnO_2)^{2+}$. For the sake of clarity, the orbitals are described using their symmetry labels σ, π, δ, φ in the $D_{\infty h}$ point group.§§ The simplicity of the d^0f^0 configuration in $(UO_2)^{2+}$ offers an ideal starting point before moving to the d^0f^2 configuration in $(PuO_2)^{2+}$ and on to the **1-An** metal complexes.

The SO-CASSPT2 calculations show that the equatorial coordination of ligands has a greater impact on **1-U** than **1-Pu** in terms of composition and assignment of their low-lying states with respect to the $(AnO_2)^{2+}$ models, see ESI for more detailed information on the uranyl system.

Given the $5f^2$ configuration of $(PuO_2)^{2+}$ and **1-Pu**, the ground state term symbol of $^3H_{4g}$ was confirmed to be correct due to the equal occupation the $5f_\delta$ and $5f_\varphi$ orbitals. The position and assignment of the excited states were similar in both systems where triplet states predominate up to ~12,000 cm^{-1} (~830 nm). Excitations at higher energy which mainly correspond to singlet configurations appear at ~16,000 cm^{-1} (~625 nm), **Fig. 3, Tables S1 & S2**.

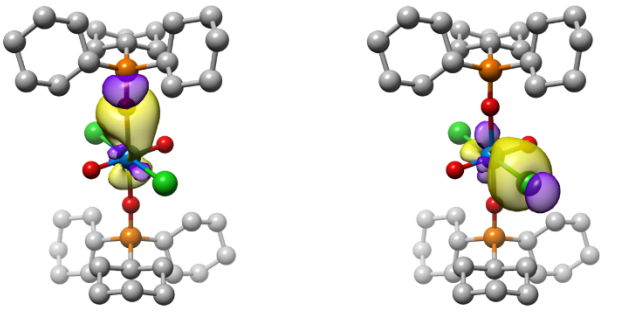

Fig. 2. Selected NLMOs in the equatorial plane of **1-U** and **1-Pu**.

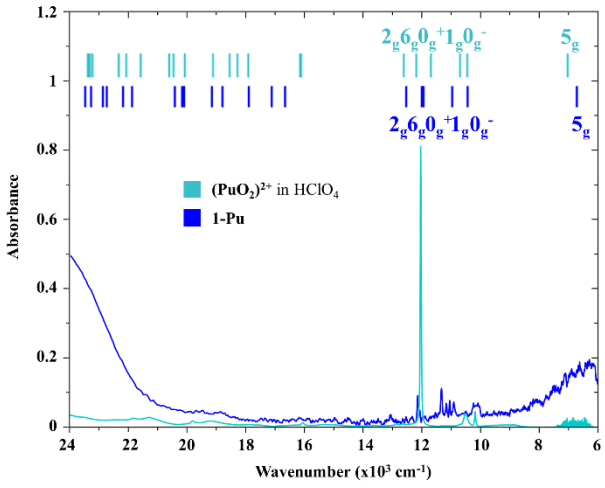

Fig. 3. Solution phase UV-vis-NIR spectrum of $(PuO_2)^{2+}$ in 1M $HClO_4$ (calypso trace) and solid-state spectrum of **1-Pu** (blue trace), at ambient temperature, with vertical bars corresponding to the SO-PT2 calculated states of the respective complexes.

Although the ground state and excitations of $(PuO_2)^{2+}_{(aq)}$ and **1-Pu** seem similar, some striking differences are observed between the solution phase UV-vis-NIR spectrum of $(PuO_2)^{2+}_{(aq)}$ and the solid-state spectrum of **1-Pu**, **Fig. 3**. Where $(PuO_2)^{2+}_{(aq)}$ features an intense Laporte forbidden excitation at ~12,039 cm^{-1} (~831 nm; ε = 555 $M^{-1}cm^{-1}$) predicted as Ω = 4g (^3H_g) → Ω = 0^+_g ($^3\prod_g$).[3, 23] Given that these electronic states have ΔJ = 2 (J = 4 and J = 2, respectively), this transition is considered to be hypersensitive in nature. Thus, the dramatic change observed in the peak at ~12,039 cm^{-1} is explained by the presence of an inversion centre in **1-Pu**, while a variety of non-centrosymmetric structures can be found in $(PuO_2)^{2+}_{(aq)}$. The non-centrosymmetric *cis*-$PuO_2Cl_2(OPcy_3)_2$ complex could exhibit the characteristic excitation at ~12,039 cm^{-1}, but a solution phase spectrum in $CDCl_3$ showed no such evidence, see **Fig. S5**. We note that the spectrum was recorded ~1 month after the synthesis was performed and showed evidence of some Pu(IV), see ESI for details.

The $OPcy_3$ ligand offers a convenient handle in ^{31}P NMR spectroscopy. Previous studies of uranyl-phosphine oxide complexes have observed *cis*/*trans* isomerization by ^{31}P NMR spectroscopy.[5, 13] Previously it was reported that $PuO_2Cl_2(OPcy_3)_2$ resonated at δ −110.2 ppm, though some of the details are uncertain.[12] In our hands, **1-Pu** displayed two paramagnetically shifted and broadened resonances at δ −5.6 and −111.0 ppm ($CDCl_3$), in an ~1:3 ratio, respectively. It is expected that a *cis* or *trans* isomer would give different shifts as observed for the uranyl analogues, the paramagnetism of the $(PuO_2)^{2+}$ ion complicates a full interpretation, in addition to experimental limitations by radiological restrictions. Previous studies of *trans*-$PuO_2Cl_2(OPPh_3)_2$, **2-Pu**, showed that only a single ^{31}P resonance at room temperature was observed, ca. δ −144.5 ppm (CD_2Cl_2), while two resonances attributed to the *cis* and *trans* isomers with little separation were observed at reduced temperature (ca. δ −185 and −187 ppm, respectively, 253 K).[7] The reaction of $[PuO_2Cl_2(THF)_2]_2$ with $OPPh_3$ showed a major resonance at δ –146 ppm (THF-d_8) which was attributed to a putative "$PuO_2Cl_2(OPPh_3)_2$" complex, while a second, smaller, resonance was observed at δ –16 ppm which was attributed to a "one to one complex" *e.g.* "$[PuO_2Cl_2(OPPh_3)(THF)_x]_n$."[24] When an excess of $OPcy_3$ in $CDCl_3$ was added to **1-Pu**, not only were the two resonances still present at approximately the same shifts, but a third resonance at δ +55.4 ppm was observed, this value is near the value of free $OPcy_3$, δ +50.574 ppm ($CDCl_3$).[10]

Conclusions

In summary the synthesis of *trans*-$PuO_2Cl_2(OPcy_3)_2$, **1-Pu**, has been confirmed, crystallizing as a distorted octahedron with all homo ligands trans to one another, and offers a good structural comparison with its uranyl analogue, **1-U**. Theoretical calculations show that the coordination of meridional ligands gives a larger effect on the axial An≡O_{yl} interaction for **1-U** than for **1-Pu**. This claim of bond weaking is supported by both bonding and electronic structure analysis. Furthermore, QTAIM results showed that despite the prediction of higher covalency in the An–Cl bonds, the An–O_P bonds are stronger based on the accumulation of electron density in the interatomic region. Due to the crystallographic inversion centre, the intense ^3H_g (J = 4) → $^3\prod_g$ (J = 2) transition (hypersensitive) characteristic of $(PuO_2)^{2+}_{(aq)}$ is significantly decreased in **1-Pu**. Characterization of **1-Pu** by ^{31}P NMR spectroscopy was in line with other examples of $(PuO_2)^{2+}$/phosphine oxide complexes. This work highlights the subtleties involved with calculating bonding in the actinyl ions, and the necessity for a careful approach to interpretation.

Acknowledgements and Conflict of Interest

We thank the support of the U.S. Department of Energy, Office of Science, Office of Basic Energy Sciences, Heavy Element Chemistry program under Award Number DE-FG02-13ER16414 (TEAS), Los Alamos National Laboratory – Laboratory Directed Research and Development funding for a J. Robert Oppenheimer Distinguished Postdoctoral Fellowship (CAPG), New Mexico State University Startup Funds (CJW), and the Royal Society for a University Research Fellowship (CAPG). The isotopes used in this research were supplied by the U.S. Department of Energy Isotope Program, managed by the Office of Science for Nuclear Physics. We thank Dr. Bonnie Klamm for assistance with the ozone experiment as well as Mr. Jason Johnson and Ms. Ashley Gray for radiological assistance. The authors declare no competing financial interest.

Notes and references

§ A perfectly a cylindrical single or triple bond has ε(r) ~0.

§§ In this symmetry the spectroscopic terms are often denoted as $^{2S+1}\Lambda_{\Omega(g/u)}$, where Λ and Ω are projections of the orbital (L) and total (J) angular momentum onto the nuclear axis. They are defined as $\Lambda = |M_L|$ and $\Omega = \Lambda + M_S$.

1. L. L. Burger, *J. Phys. Chem.*, 1958, **62**, 590-593.
2. E. R. Bertelsen, M. R. Antonio, M. P. Jensen and J. C. Shafer, *Solvent Extr. Ion Exch.*, 2021, *ASAP*. DOI: 10.1080/07366299.2021.1920674
3. L. R. Morss, N. M. Edelstein and J. Fuger, *The Chemistry of the Actinide and Transactinide Elements*, Springer, Dordrecht, The Netherlands, 4th edn., 2010.
4. G. H. John, I. May, M. J. Sarsfield, H. M. Steele, D. Collison, M. Helliwell and J. D. McKinney, *Dalton Trans.*, 2004, 734-740.
5. M. J. Sarsfield, I. May, S. M. Cornet and M. Helliwell, *Inorg. Chem.*, 2005, **44**, 7310-7312.
6. N. W. Alcock, M. M. Roberts and D. Brown, *Dalton Trans.*, 1982, 25-31.
7. C. Berthon, N. Boubals, I. A. Charushnikova, D. Collison, S. M. Cornet, C. Den Auwer, A. J. Gaunt, N. Kaltsoyannis, I. May, S. Petit, M. P. Redmond, S. D. Reilly and B. L. Scott, *Inorg. Chem.*, 2010, **49**, 9554-9562.
8. I. A. Charushnikova, N. N. Krot, Z. A. Starikova and I. N. Polyakova, *Radiochemistry*, 2007, **49**, 464-469.
9. I. A. Charushnikova, N. N. Krot and Z. A. Starikova, *Radiochemistry*, 2007, **49**, 561-564.
10. C. J. Windorff, C. Celis-Barros, J. M. Sperling, N. C. McKinnon and T. E. Albrecht-Schmitt, *Chem. Sci.*, 2020, **11**, 2770-2782.
11. A. W. G. Platt, *Coord. Chem. Rev.*, 2017, **340**, 62-78.
12. S. M. Cornet, I. May, M. J. Sarsfield, N. Kaltsoyannis, J. Haller, C. D. Auwer and D. Meyer, *J. Alloys Comp.*, 2007, **444–445**, 453-456.

13. L. J. L. Häller, N. Kaltsoyannis, M. J. Sarsfield, I. May, S. M. Cornet, M. P. Redmond and M. Helliwell, *Inorg. Chem.*, 2007, **46**, 4868-4875.
14. G. Bombieri, E. Forsellini, J. P. Day and W. I. Azeez, *Dalton Trans.*, 1978, 677-680.
15. S. B. Akona, J. Fawcett, J. H. Holloway, D. R. Russell and I. Leban, *Acta Cryst.*, 1991, **C47**, 45-48.
16. J. I. Bullock, *J. Inorg. Nucl. Chem.*, 1967, **29**, 2257-2264.
17. R. F. W. Bader, in *The Quantum Theory of Atoms in Molecules*, eds. C. F. Matta and R. J. Boyd, Wiley-VCH Verlag GmbH & Co. KGaA 2007, ch. 2, pp. 35-59.
18. E. Espinosa, I. Alkorta, J. Elguero and E. Molins, *J. Chem. Phys.*, 2002, **117**, 5529-5542.
19. D. Cremer and E. Kraka, *Angew. Chem., Int. Ed.*, 1984, **23**, 627-628.
20. C. Madic, D. E. Hobart and G. M. Begun, *Inorg. Chem.*, 1983, **22**, 1494-1503.
21. D.-C. Sergentu, T. J. Duignan and J. Autschbach, *J. Phys. Chem. Lett.* , 2018, **9**, 5583-5591.
22. R. G. Denning, *J. Phys. Chem. A*, 2007, **111**, 4125-4143.
23. S. Matsika, R. M. Pitzer and D. T. Reed, *J. Phys. Chem. A*, 2000, **104**, 11983-11992.
24. A. J. Gaunt, S. D. Reilly, T. W. Hayton, B. L. Scott and M. P. Neu, *Chem. Commun.*, 2007, 1659-1661.